

MEASUREMENTS OF ANISOTROPY IN THE COSMIC MICROWAVE BACKGROUND RADIATION AT 0°5 SCALES NEAR THE STARS HR 5127 AND ϕ HERCULIS

S. T. TANAKA,^{1,2} A. C. CLAPP,^{1,2,3} M. J. DEVLIN,^{1,2,4} N. FIGUEIREDO,^{1,5,6} J. O. GUNDERSEN,^{1,5} S. HANANY,^{1,2}
V. V. HRISTOV,^{1,2} A. E. LANGE,^{1,3} M. A. LIM,^{1,5} P. M. LUBIN,^{1,5} P. R. MEINHOLD,^{1,5}
P. L. RICHARDS,^{1,2} G. F. SMOOT,^{1,2,7} AND J. STAREN^{1,5}

Received 1995 December 12; accepted 1996 June 27

ABSTRACT

We present measurements of cosmic microwave background (CMB) anisotropy near the stars HR 5127 and ϕ Hercules from the fifth flight of the Millimeter-wave Anisotropy eXperiment (MAX). We scanned 8° strips of the sky with an approximately Gaussian 0°5 FWHM beam and a 1°4 peak to peak sinusoidal chop. The instrument has four frequency bands centered at 3.5, 6, 9, and 14 cm⁻¹. The *IRAS* 100 μ m map predicts that these two regions have low interstellar dust contrast. The HR 5127 data are consistent with CMB anisotropy. The ϕ Hercules data, which were measured at lower flight altitudes, show time variability at 9 and 14 cm⁻¹, which we believe to be due to atmospheric emission. However, the ϕ Hercules data at 3.5 and 6 cm⁻¹ are essentially independent of this atmospheric contribution and are consistent with CMB anisotropy. Confusion from Galactic foregrounds is unlikely based on the spectrum and amplitude of the structure at these frequencies. If the observed HR 5127 structure and the atmosphere-independent ϕ Hercules structure are attributed to CMB anisotropy, then we find $\Delta T/T = \langle l(l+1)C_l/2\pi \rangle^{1/2} = 1.2^{+0.4}_{-0.3} \times 10^{-5}$ for HR 5127 and $1.9^{+0.7}_{-0.4} \times 10^{-5}$ for ϕ Hercules in the flat band approximation. The upper and lower limits represent a 68% confidence interval added in quadrature with a 10% calibration uncertainty.

Subject headings: cosmic microwave background — cosmology: observations

1. INTRODUCTION

Measurements of the anisotropy of the cosmic microwave background (CMB) provide an effective method for constraining models of large-scale structure formation. Standard inflationary models predict a Doppler peak at angular scales $\lesssim 1^\circ$. The Millimeter-wave Anisotropy eXperiment (MAX) measures anisotropy on 0°5 angular scales. MAX has presented CMB results for six sky regions from four previous flights: MAX1 (Fischer et al. 1992), MAX2 (Alsop et al. 1992), MAX3 (Meinhold et al. 1993a; Gundersen et al. 1993; Fischer et al. 1995), and MAX4 (Clapp et al. 1994; Devlin et al. 1994). Several other ground-based and balloon-borne experiments have also reported detections at these angular scales (de Bernardis et al. 1994; Gundersen et al. 1995; Netterfield et al. 1995; Ruhl et al. 1995; Cheng et al. 1996). In this paper we report on two new CMB observations from the fifth flight of MAX (MAX5).

2. INSTRUMENT

The instrument has been described in detail elsewhere (Fischer et al. 1992; Alsop et al. 1992; Meinhold et al. 1993b). MAX is an off-axis Gregorian telescope with a bolometric photometer mounted on an attitude-controlled balloon plat-

form. The telescope has a 1 m parabolic primary and an elliptical secondary that sinusoidally modulates the beam in azimuth at 5.4 Hz with a 1°4 peak-to-peak throw. The underfilled optics provide an approximately Gaussian 0°5 FWHM beam. An adiabatic demagnetization refrigerator cooled the single-pixel, four-band photometer to 85 mK. The frequency bands were centered at 3.5, 6, 9, and 14 cm⁻¹ with respective fractional bandwidths 0.5, 0.5, 0.4, and 0.2. The ratio of 2.726 K thermodynamic temperature to antenna temperature in each frequency band is 1.62, 2.50, 6.66, and 38.7, respectively.

3. OBSERVATION

The instrument was launched from the National Scientific Balloon Facility in Palestine, Texas, at 1.16 UT 1994 June 20. The observation altitude drifted from 35 to 32 km. Each CMB anisotropy observation consists of constant velocity scans in azimuth of $\pm 4^\circ$ while optically tracking a target star such that sky rotation pivots the observed area about the star. At the center of the scan, the target star is offset 0°55 into one lobe of the chopped beam pattern. The three MAX5 target stars are HR 5127, ϕ Hercules, and μ Pegasi. Lim et al. (1996) report on the μ Pegasi observation. We report here the results for the sky regions near HR 5127 ($\alpha = 13^{\text{h}}37^{\text{m}}7$, $\delta = 36^\circ19'$) and ϕ Hercules ($\alpha = 16^{\text{h}}08^{\text{m}}6$, $\delta = 44^\circ57'$; epoch 1994).

We chose the HR 5127 and ϕ Hercules regions for low *IRAS* 100 μ m dust contrast (Wheelock et al. 1994) and the absence of known extragalactic radio sources (Herbig & Readhead 1992). We observed the HR 5127 region from 5.99 to 6.97 UT and the ϕ Hercules region from 8.29 to 8.91 UT. We calibrated the instrument before and after each observation using a membrane transfer standard (Fischer et al. 1992).

We observed Jupiter from 4.86 to 4.95 UT to measure the beam size. We confirm the membrane calibration using the

¹ NSF Center for Particle Astrophysics, Berkeley, CA 94720.

² Physics Department, University of California at Berkeley, Berkeley, CA 94720.

³ Division of Physics, Mathematics, and Astronomy, California Institute of Technology, Pasadena, CA 91125.

⁴ Present address: Department of Physics, Princeton University, Princeton, NJ 08544.

⁵ Physics Department, University of California at Santa Barbara, Santa Barbara, CA 93106.

⁶ Escola Federal de Engenharia de Itajubá, 37500-000 Itajubá, MG, Brazil; Instituto Nacional de Pesquisas Espaciais, 12201-970 São José dos Campos, SP, Brazil.

⁷ Physics Division, Lawrence Berkeley Laboratory, Berkeley, CA 94720.

best-fit beam size and the temperature of Jupiter (Griffin et al. 1986). We assume a 10% uncertainty in calibration. The calibration is such that a chopped beam centered between sky regions with temperatures T_1 and T_2 would yield $\Delta T = T_1 - T_2$ in the absence of instrumental noise.

Anisotropy experiments are potentially susceptible to off-axis response to local sources. We measured the unchopped off-axis response in the 3.5 cm^{-1} band to be $\geq 70 \text{ dB}$ below the on-axis response at angles from 15° to 25° in elevation above the bore sight. We have not made comparable measurements of the chopped sidelobe response in azimuth. Our strongest argument against sidelobe contamination is that the observed structure is stationary on the sky while the horizon and local foregrounds shift. The elevation of the observation changes from 42° to 31° and from 46° to 39° for HR 5127 and ϕ Herculis, respectively. Sidelobe response from the Earth and the balloon should change over time. To minimize sidelobe response from the Moon, we observe when the Moon is not full. The Moon was $\sim 56^\circ$ away from HR 5127 and $\sim 66^\circ$ away from ϕ Herculis.

4. DATA ANALYSIS

4.1. Data Reduction

We exclude $\sim 15\%$ of the data in the removal of transients due to cosmic rays (Alsop et al. 1992). We demodulate the detector output using the sinusoidal reference from the chopping secondary to produce antenna temperature differences ΔT_A on the sky. The demodulation produces data sets in phase and 90° out of phase with the optical signal as defined by the calibration. The noise averaged over the observations gives respective CMB sensitivities of 590, 270, 620, and $4800 \mu\text{K s}^{1/2}$ for HR 5127 and 600, 300, 630, and $4800 \mu\text{K s}^{1/2}$ for ϕ Herculis in the 3.5 , 6 , 9 , and 14 cm^{-1} bands. The slight differences in sensitivities are due to long timescale drifts in instrument gain.

The signal in each band is offset from zero for both observations because of chopped primary mirror emissivity differences and chopped atmospheric emission. The mean instrumental offsets in antenna temperature were 0.7, 0.2, 1.5, and 3.0 mK in the 3.5 , 6 , 9 , and 14 cm^{-1} bands. The offset fluctuates with a period of $\sim 300 \text{ s}$ and amplitudes of $200 \mu\text{K}$ and $300 \mu\text{K}$ at 9 and 14 cm^{-1} . We subtract the offset and offset drift with a linear least-squares fit to each 72 s half-scan from 0° to $\pm 4^\circ$ to 0° . This method removes the $\sim 300 \text{ s}$ fluctuations as long as the fluctuations are not phase-synchronous with the scan period. The residual temporal correlation between frequency bands is a few percent.

For each observation, we calculate the means and 1σ uncertainties of the ΔT_A for 29 pixels separated by $17'$ on the sky. The uncertainties are consistent with the integration time and the Gaussian random instrument noise. Figure 1 shows the measured ΔT_A for the HR 5127 observation. There is significant signal that is not consistent with Gaussian random instrument noise. (Reduced χ^2 for the null hypothesis = 64/29, 94/29, 49/29, and 31/29 at 3.5 , 6 , 9 , and 14 cm^{-1} .) By comparison, the out of phase components are consistent with Gaussian random instrument noise. (Reduced $\chi^2 = 20/29$, 18/29, 36/29, and 27/29 at 3.5 , 6 , 9 , and 14 cm^{-1} .) There is correlated structure in the 3.5 , 6 , and 9 cm^{-1} bands and no significant signal at 14 cm^{-1} as expected for CMB anisotropy. If we divide the observation into two equal time periods, the differences between the two halves are consistent with zero in the main CMB bands. (Reduced $\chi^2 = 20/29$, 26/29, and 28/29 at 3.5 , 6 , and 9 cm^{-1} .)

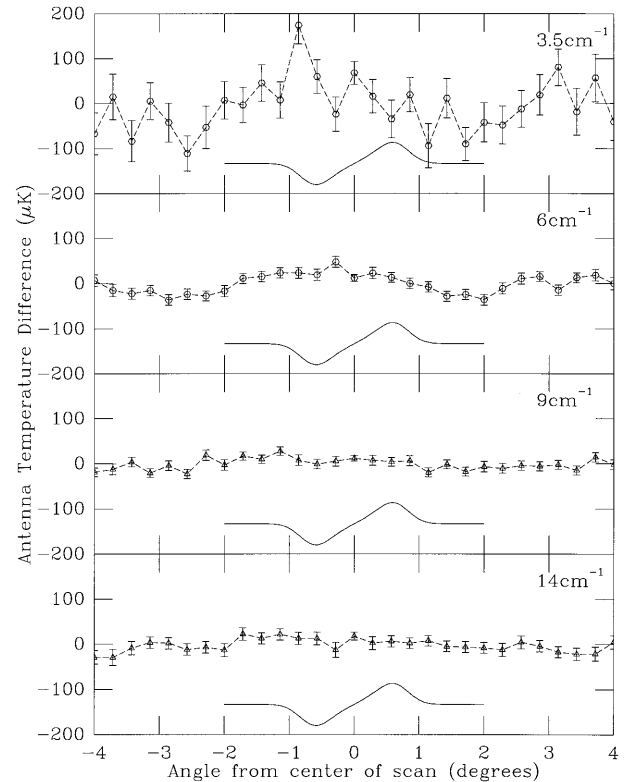


FIG. 1.—Antenna temperature differences ($\pm 1 \sigma$) for the data near HR 5127. The points are separated by $17'$ in azimuth. The solid lines show the response to a point source in each of the bands.

The temporal stability of the signal in each pixel suggests that the signal is not due to either sidelobe response or atmospheric emission.

Figure 2 shows the measured ΔT_A for the ϕ Herculis observation. There is significant signal that is not consistent with Gaussian random instrument noise. (Reduced $\chi^2 = 49/29$, 156/29, 86/29, and 77/29 at 3.5 , 6 , 9 , and 14 cm^{-1} .) By comparison, the out of phase components are consistent with Gaussian random instrument noise. (Reduced $\chi^2 = 42/29$, 38/29, 15/29, and 35/29 at 3.5 , 6 , 9 , and 14 cm^{-1} .) In addition to the correlated structure at 3.5 , 6 , and 9 cm^{-1} , there is structure at 14 cm^{-1} . If we divide the observation into two equal time periods, the differences between the two halves are consistent with zero at 3.5 and 6 cm^{-1} (reduced $\chi^2 = 21/29$ and 22/29), suggesting that the signal is neither sidelobe response nor atmospheric emission. We interpret the time variable structure at 9 and 14 cm^{-1} as atmosphere (reduced $\chi^2 = 34/29$ and 55/29).

4.2. Spectral Discrimination

In order to test the hypothesis that the signals in all frequency bands originate from a single morphology, we determined a best-fit sky model y_i by minimizing

$$\chi^2 = \sum_{j=1}^4 \sum_{i=1}^{29} (x_{ij} - a_j y_i)^2 / \sigma_{ij}^2, \quad (1)$$

where x_{ij} and σ_{ij} are the measured mean and uncertainty in angular bin i for frequency band j . The a_j denote the set of

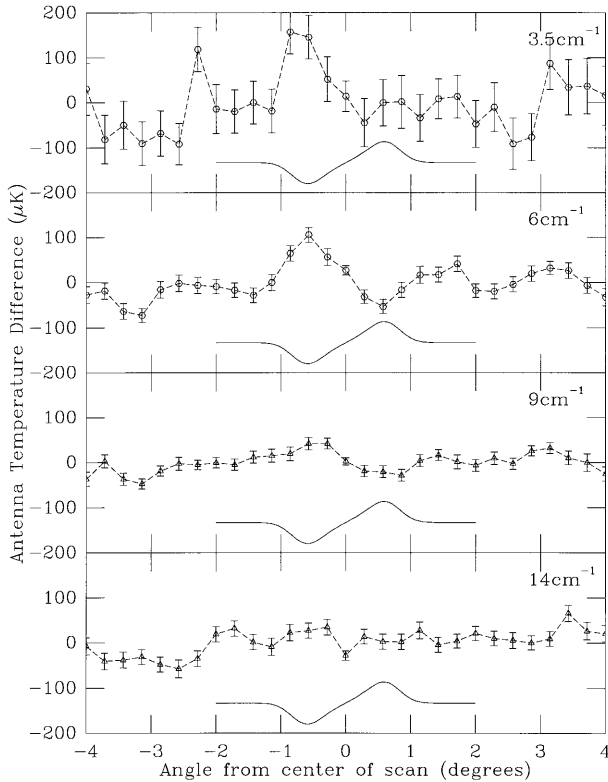


FIG. 2.—Antenna temperature differences ($\pm 1 \sigma$) for the data near ϕ Herculis. The points are separated by $17'$ in azimuth. The solid lines show the response to a point source in each of the bands.

scale factors for an astrophysical process. Table 1 gives reduced χ^2 using scale factors a_i for CMB, free-free, synchrotron, and dust emission. The HR 5127 data set is spectrally consistent with free-free, synchrotron, and CMB emission. The complete ϕ Herculis data set is not spectrally consistent with any of the processes. However, the ϕ Herculis data at 3.5 and 6 cm^{-1} are spectrally inconsistent with synchrotron emission and spectrally consistent with free-free, dust, and CMB emission.

4.3. Galactic and Extragalactic Emission

At 6 , 9 , and 14 cm^{-1} , the predominant astrophysical source of confusion is thermal emission from interstellar dust. Using a brightness scaling for high-latitude dust (Meinhold et al. 1993a; Fischer et al. 1995), we can extrapolate the *IRAS* $100 \mu\text{m}$ data (Wheelock et al. 1994) to our frequency bands. At most, we expect the differential dust emission to contribute a few microkelvins in antenna temperature at 14 cm^{-1} and

negligibly at lower frequencies in both HR 5127 and ϕ Herculis. The observed 14 cm^{-1} structure in ϕ Herculis does not correlate with the structure obtained by convolving our beam and scan pattern with the *IRAS* $100 \mu\text{m}$ map.

The Herbig & Readhead (1992) catalog has no bright radio sources in either region. The convolution of our scan pattern with the $30' \times 30'$ smoothed 408 MHz Haslam et al. (1982) map sets conservative amplitude limits on free-free and synchrotron emission. Assuming antenna temperature scales as ν^β , we obtain $\lesssim 1\%$ and $\lesssim 10\%$ of the observed structure at 3.5 cm^{-1} for synchrotron ($\beta = -2.7$) and free-free emission ($\beta = -2.1$), respectively.

4.4. Atmosphere

During the ϕ Herculis observation the balloon altitude dropped to 32 km . Altitude fluctuations of $\sim 50 \text{ m}$ every $\sim 300 \text{ s}$ correlate with $\sim 300 \mu\text{K}$ detector offset fluctuations at 14 cm^{-1} . If we process the balloon altitude like a detector signal, removing offset and offset drift for each half-scan and calculating a mean for each azimuth bin, we find that the 14 cm^{-1} structure in ϕ Herculis correlates with the binned balloon altitude with a linear correlation coefficient $R = -0.68$, suggesting that the observed structure is due to atmospheric contamination. We expect to observe less atmospheric emission during the HR 5127 observation because the average balloon altitude was 35 km .

If all the structure at 14 cm^{-1} is attributed to modeled atmospheric contamination (Airhead Software, Boulder, CO), we obtain $< 5\%$ and $< 10\%$ of the observed structure at 3.5 and 6 cm^{-1} , respectively. The structure at 3.5 and 6 cm^{-1} is also less correlated with the binned balloon altitude ($R = -0.09$ and -0.17). In our CMB analysis of ϕ Herculis, we consider only the 3.5 and 6 cm^{-1} data. An alternative analysis that considers the linear combinations of all frequency band data orthogonal to the atmospheric contamination yields the same CMB anisotropy confidence intervals within 5% . Similar analyses have been used to separate CMB from other astrophysical sources (Dodelson & Stebbins 1994).

5. DISCUSSION

We model the anisotropy with a correlation function $\langle \Delta T(x_1) \Delta T(x_2) \rangle = C_0 c(\theta)$, using a likelihood ratio statistic to set limits on the amplitude of the fluctuations $C_0^{1/2}$ (Cheng et al. 1994). We include correlations between frequency bands in the covariance matrix. However, the off diagonal elements affect the calculated values of $C_0^{1/2}$ by $\lesssim 2\%$.

To set limits on the CMB anisotropy, we include the 3.5 , 6 , and 9 cm^{-1} data for the HR 5127 observation and the 3.5 and 6 cm^{-1} data for the ϕ Herculis observation. Assuming a

TABLE 1
SPECTRAL CONSTRAINTS^a

Observation	CMB	Free-Free ^b	Synchrotron ^c	Dust ^d
HR 5127	97/87	92/87	100/87	136/87
ϕ Herculis.....	119/87	132/87	164/87	170/87
ϕ Herculis (3.5 and 6 cm^{-1} only).....	25/29	36/29	50/29	29/29

^a Reduced χ^2 from eq. (1), using a_i for different astrophysical processes. Calibration uncertainty included.

^b Assumes brightness $I_\nu \propto \nu^{-0.1}$.

^c Assumes $I_\nu \propto \nu^{-0.7}$.

^d Assumes $I_\nu \propto \nu^{1.4} B_\nu(T = 18 \text{ K})$, where B_ν is the Planck function.

TABLE 2
MAX5 AND REANALYZED MAX4 LIMITS ON CMB ANISOTROPY

Observation	GACF $\Delta T/T_{\text{CMB}}$	Flat Band $\langle l(l+1)C_l/2\pi \rangle^{1/2}$
HR 5127	$1.8^{+0.6}_{-0.5} \times 10^{-5}$	$1.2^{+0.4}_{-0.3} \times 10^{-5}$
ϕ Hercules.....	$2.9^{+1.0}_{-0.7} \times 10^{-5}$	$1.9^{+0.7}_{-0.4} \times 10^{-5}$
GUM.....	$3.1^{+1.2}_{-0.8} \times 10^{-5}$	$2.0^{+0.6}_{-0.4} \times 10^{-5}$
ι Draconis.....	$2.6^{+1.3}_{-0.8} \times 10^{-5}$	$1.7^{+0.8}_{-0.5} \times 10^{-5}$
σ Hercules.....	$2.8^{+1.2}_{-0.9} \times 10^{-5}$	$1.8^{+0.8}_{-0.6} \times 10^{-5}$

NOTE.—Upper and lower limits represent 68% confidence interval added in quadrature with 10% calibration uncertainty.

Gaussian 0.5° FWHM beam, we present two measures of the fluctuations in Table 2 for each observation. We find the 68% confidence interval for $C_0^{1/2}$ for a Gaussian correlated sky $c(\theta) = \exp(-\theta^2/2\theta_c^2)$ where $\theta_c = 25'$ (GACF). The central value represents the $C_0^{1/2}$ for which the cumulative distribution function equals 50%. We also find a flat band power estimate $\langle l(l+1)C_l/2\pi \rangle^{1/2}$ for $c(\theta) = (1/4\pi) \sum (2l+1)C_l P_l(\cos \theta)$ where $C_l \propto 1/l(l+1)$.

Table 2 also lists MAX4 CMB anisotropy results. The GACF limits are as much as 20% lower than previously published (Clapp et al. 1994; Devlin et al. 1994). The previous MAX4 analyses did not include sufficient power in the off-diagonal elements and improperly normalized the larger beam sizes in the theoretical covariance matrix. The distributed data sets have not changed.

Bayesian analyses and likelihood ratio analyses of the MAX4 and MAX5 data sets yield similar $\Delta T/T$ confidence intervals except for σ Hercules. The 68% confidence interval GACF $\Delta T/T$ for σ Hercules is $4.0^{+1.7}_{-1.1} \times 10^{-5}$ for a Bayesian analysis and $2.8^{+1.2}_{-0.9} \times 10^{-5}$ for a likelihood ratio analysis. The discrepancy between the two analyses is being investigated.

6. CONCLUSION

We have presented new MAX measurements of CMB anisotropy with high sensitivity at 0.5° angular scales. The amplitude and morphology of the observed structure is not consistent with known forms of interstellar dust, synchrotron, and free-free emission. The HR 5127 data are consistent with CMB anisotropy with flat band power $\Delta T/T = 1.2^{+0.4}_{-0.3} \times 10^{-5}$. The ϕ Hercules data are consistent with CMB anisotropy with flat band power $\Delta T/T = 1.9^{+0.7}_{-0.4} \times 10^{-5}$ if we consider linear combinations of the data that are independent of the atmospheric emission spectrum or only the 3.5 and 6 cm^{-1} data. The upper and lower limits represent a 68% confidence interval added in quadrature with a 10% calibration uncertainty. The difference between the HR 5127 and ϕ Hercules results is similar to the difference between the previously reported results for the sky regions near μ Pegasi (Meinhold et al. 1993a) and γ Ursae Minoris (Alsop et al. 1992; Gundersen et al. 1993; Devlin et al. 1994). The HR 5127 and ϕ Hercules data are available from the authors.

This work was supported by the National Science Foundation through the Center for Particle Astrophysics (cooperative agreement AST 91-20005), the National Aeronautics and Space Administration under grants NAGW-1062 and FD-NAGW-2121, the University of California, and previously the California Space Institute. N. F. was partially supported by Conselho Nacional de Desenvolvimento Científico e Tecnológico, Brazil. We would like to thank O. Levy for his assistance with the flight preparation, the MSAM team for borrowed equipment and discussions, and M. White.

REFERENCES

- Alsop, D. C., et al. 1992, *ApJ*, 395, 317
 Cheng, E. S., et al. 1994, *ApJ*, 422, L37
 ———. 1996, *ApJ*, 456, L71
 Clapp, A. C., et al. 1994, *ApJ*, 433, L57
 de Bernardis, P., et al. 1994, *ApJ*, 422, L33
 Devlin, M. J., et al. 1994, *ApJ*, 430, L1
 Dodelson, S., & Stebbins, A. 1994, *ApJ*, 433, 440
 Fischer, M. L., et al. 1992, *ApJ*, 388, 242
 ———. 1995, *ApJ*, 444, 226
 Griffin, M. J., et al. 1986, *Icarus*, 65, 244
 Gundersen, J. O., et al. 1993, *ApJ*, 413, L1
 ———. 1995, *ApJ*, 443, L57
 Haslam, C. G. T., et al. 1982, *A&AS*, 47, 1
 Herbig, T., & Readhead, A. C. S. 1992, *ApJS*, 81, 83
 Lim, M. A., et al. 1996, *ApJ*, submitted
 Meinhold, P. R., et al. 1993a, *ApJ*, 409, L1
 ———. 1993b, *ApJ*, 406, 12
 Netterfield, C. B., Jarosik, N., Page, L., Wilkinson, D., & Wollack, E. 1995, *ApJ*, 445, L69
 Ruhl, J. E., Dragovan, M., Platt, S. R., Kovac, J., & Novak, G. 1995, *ApJ*, 453, L1
 Wheelock, S. L., et al. 1994, *IRAS Sky Survey Atlas Explanatory Supplement*, JPL Publication 94-11 (Pasadena: JPL)